Pertanika J. Sci. & Technol. 33 (1): 465 - 489 (2025)

PERTANIKA JOURNALS

SCIENCE & TECHNOLOGY

Journal homepage: http://www.pertanika.upm.edu.my/

Rice Extent and Cropping Patterns in Terengganu Malaysia Based on Sentinel-2 Data on Google Earth Engine

Fatchurrachman[1], Norhidayah Che Soh[1], Ramisah Mohd Shah[1], Frisa Irawan Ginting[1], Sunny Goh Eng Giap[2], Muhammad Nazir Siham[3] and Rudiyanto[1]*

[1]Program of Crop Science, Faculty of Fisheries and Food Science, Universiti Malaysia Terengganu, Kuala Nerus 21030, Terengganu, Malaysia
[2]Program of Environmental Technology, Faculty of Ocean Engineering Technology, Universiti Malaysia Terengganu, 21030 Kuala Nerus, Terengganu, Malaysia
[3]Malaysian Remote Sensing Agency, Ministry of Energy, Science, Technology, Environment and Climate Change, No 13, Jalan Tun Ismail, 50480, Kuala Lumpur, Malaysia

ABSTRACT

Rice is a vital staple food in Malaysia, with consumption of 2.7 million MT in 2016, forecasted to rise to 3.5 million MT by 2026. To address food security, the Malaysian government targets a 70% self-sufficiency level (SSL) in rice production, requiring precise spatiotemporal information on rice cultivation. Remote sensing has been widely used to map rice extent in Malaysia, particularly in granary areas (facilitated by irrigation system), the main production zones. However, studies on non-granary areas (without irrigation systems) remain limited. This study addresses this gap by employing the Phenology-Expert Based Unsupervised Classification Method (PEB-UC) with Sentinel-2 time series data on the Google Earth Engine platform to map rice extent and cropping patterns at the sub-district level across Terengganu State, Malaysia, covering both granary and non-granary areas. The results revealed scattered rice parcels totalling 8,184 ha, with 4,377 ha in the IADA KETARA granary area (Besut District) and 3,807 ha in non-granary areas. The maps showed a relative discrepancy of -29.15% with agricultural statistics but demonstrated a strong correlation at the district level ($R^2 = 0.99$; RMSE = 632 ha). Validation of PEB-UC achieved an overall accuracy of 0.979 and a kappa coefficient of 0.957, outperforming Random Forest (RF) and Support Vector Machine (SVM) models. The PEB-UC rice map displayed denser, clearer separability between rice and non-rice compared to supervised models, as shown in

ARTICLE INFO

Article history:
Received: 05 April 2024
Accepted: 03 September 2024
Published: 27 January 2025

DOI: https://doi.org/10.47836/pjst.33.1.21

E-mail addresses:
p5844@pps.umt.edu.my (Fatchurrachman)
norhidayah.soh@umt.edu.my (Norhidayah Che Soh)
ramisah@umt.edu.my (Ramisah Mohd Shah)
p5277@pps.umt.edu.my (Frisa Irawan Ginting)
sunnyg@umt.edu.my (Sunny Goh Eng Giap)
nazirsiham@remotesensing.gov.my (Muhammad Nazir Siham)
rudiyanto@umt.edu.my (Rudiyanto)
* Corresponding author

ISSN: 0128-7680
e-ISSN: 2231-8526

the comparison map at https://rudiyanto.users.earthengine.app/view/riceterengganu. This study provides valuable insights into rice cultivation in Terengganu State and supports efforts to enhance food security.

Keywords: Cropping pattern, Google earth engine, harvested area, paddy rice map, phenology, Sentinel-2

INTRODUCTION

Rice serves as a primary dietary component across Southeast Asia (SEA), including Malaysia. In 2016, the consumption of rice in Malaysia amounted to 80 kilograms per capita, totalling 2.7 million metric tons of rice consumed. The annual consumption of rice in Malaysia is on the rise and is forecasted to reach 3.5 million MT by 2026 (Omar et al., 2019). In response to the national food security issue, the Malaysian government, through the *Rancangan Malaysia Ke-12* (12th Malaysia Plan), has set a goal of attaining a self-sufficiency level (SSL) of 75% for domestic rice production, equivalent to 3 million metric tons by 2025 (Ministry of Economy Malaysia, 2023).

Malaysia's rice production management is divided into two categories: rice production managed by rice granary agencies (i.e., completed by irrigation system) and rice production outside the agencies (i.e., without irrigation system). Rice granary agencies dominate Malaysia's domestic rice production, constituting approximately 70% of the total supply (Omar et al., 2019).

Terengganu is one of the rice-producing regions in Malaysia. Although it is not the main rice producer in Malaysia, Terengganu has one of the granary areas with the highest yield, IADA KETARA, reaching up to 5.4 tons per hectare. Additionally, Terengganu contributes to national rice production through granary and non-granary areas (Department of Agriculture Peninsular Malaysia, 2021).

In order to achieve the SSL rice target, it is essential to gain precise and current information regarding the geographical distribution and quantity of rice cultivation areas. In the last decades, remote sensing technology has emerged as an efficient tool to provide spatiotemporal information for crop monitoring, including rice. Remote sensing offers a cost-effective method for monitoring crops at regional and national scales, as it facilitates the rapid retrieval of spatially distributed information over large areas. In contrast to field surveys, which are often time-consuming, lack geographical details and are also costly (Omia et al., 2023; Wang et al., 2024).

Rice has highly dynamic changes in growth stages to differentiate rice from other crops and land covers, in which time series imagery data are required (Ni et al., 2021; Rudiyanto et al., 2019). Moreover, the characteristics of rice fields in SEA typically consist of small blocks, averaging less than 1 ha, necessitating high-resolution imagery data (Fatchurrachman et al., 2022; Setiyono et al., 2018). Sentinel-2A and 2B satellites

constellation, which are equipped with multispectral instruments (MSI), offer imagery data covering a range of visible, near-infrared (NIR) and short-wave infrared (SWIR) wavelengths and have high-resolution ranging from 10-60 m (depending on the selected band) (Griffiths et al., 2019; Jiang et al., 2023). These satellite imagery data also have a monthly revisit time of 5-6 times. These features of Sentinel-2 imagery data make it particularly suitable for mapping rice. Multiple studies have demonstrated the successful utilisation of Sentinel-2 imagery for mapping rice fields across diverse regions, including Bangladesh (Tiwari et al., 2024), China (Feng et al., 2023), Egypt (Ali et al., 2021), India (Raju et al., 2022), Indonesia (Rudiyanto et al., 2019), and Pakistan (Rauf et al., 2022).

Data-driven mapping algorithms, such as machine learning and deep learning, have become increasingly popular in rice mapping (Liu et al., 2022; Ramadhani et al., 2020). Despite their excellent performance, extensive ground data samples are needed to train the algorithm (Padarian et al., 2020; Thorp & Drajat, 2021; Zhao et al., 2021). Another limitation of the supervised classification is the difficulty of transferring the model due to regional or temporal differences (Qiu et al., 2024).

On the other hand, unlike the supervised methods, unsupervised methods can eliminate the need for extensive ground training samples. In particular, the k-means unsupervised method has the ability to generalise clusters from data patterns and group time series data into unique spectral responses related to rice phenology and other land uses (Ni et al., 2021; Rudiyanto et al., 2019). Thus, these advantages of the phenology unsupervised method can be used to identify rice with varying cropping calendars in Southeast Asia (Han et al., 2022).

Current studies by Han et al. (2021), Fatchurrachman et al. (2022), and Han et al. (2022) have mapped rice extent across Peninsular Malaysia using remote sensing technology. However, these maps did not provide detailed information on rice's location and planting schedule in non-granary areas. Despite non-granary areas accounting for approximately 25% of the total rice field area in Peninsular Malaysia (Department of Agriculture Peninsular Malaysia, 2021), their contribution cannot be overlooked in addressing food security issues.

Considering the existing research gap, this study's objective was to map the extent of rice cultivation and its cropping pattern in Terengganu State, Malaysia, which covers granary and non-granary areas at the sub-district level. It was accomplished through the utilisation of Sentinel-2 temporal data and phenology-expert-based unsupervised classification (PEB-UC) within the Google Earth Engine (GEE) platform. The outcomes of this study will offer crucial information on the extent of rice cultivation and its cropping schedule in Terengganu State at the Sub-district level, which can aid in addressing food security concerns.

STUDY AREA AND RICE CULTIVATION PRACTICES

Terengganu is one of the states in Malaysia located on the northeastern coast of Peninsular Malaysia (3.87° N–5.85° N and 102.37° E–103.69° E; Figure 1). Terengganu comprises seven Districts: Besut, Dungun, Kemaman, Kuala Terengganu (Kuala Nerus), Marang, Setiu, and Hulu Terengganu. Similar to other states in Peninsular Malaysia, Terengganu undergoes two monsoon seasons: the northeast monsoon (NEM), occurring from November to March, and the southwest monsoon (SWM), which lasts from May to September. Additionally, there are two short transitional periods, spanning from April to May and October to November. The NEM brings heavy rains to this region. The annual mean air temperature ranges between 26° and 28°C (Suratman et al., 2015).

The rice fields in the study area are categorised as irrigated and non-irrigated. The rice intensity in the study area is mostly a double rice cropping pattern. Planting seasons are categorised into the main season, featuring wet paddy rice cultivation from September to March, and the off-season rice crop from April to September. Locally referred to as "tanaman musim utama" and "tanaman luar musim", respectively. The off-season denotes a period marked by the lack of precipitation in the region (Hashim et al., 2022).

Terengganu has one active rice granary area: the Integrated Agriculture Development Area (IADA) Kawasan Pembangunan Pertanian Terengganu Utara (KETARA). IADA

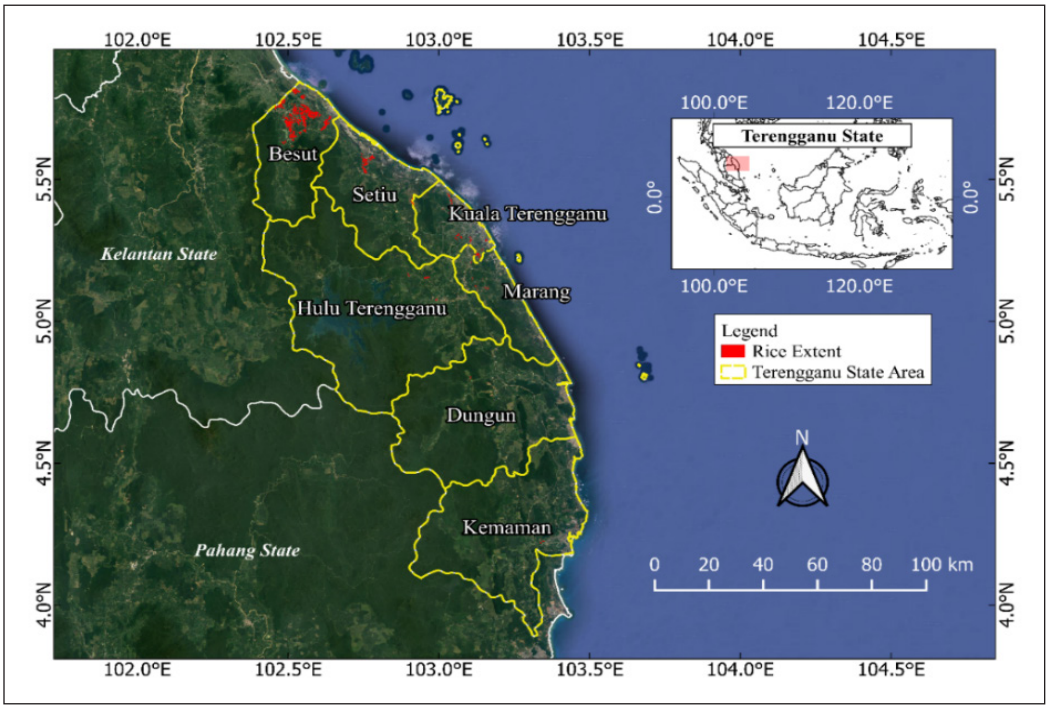

Figure 1. The study location comprises 7 Districts in Terengganu State, Malaysia. Rice extent based on this study is shown in red

KETARA is one of Malaysia's top rice producers, with yields surpassing 5.0 to 5.4 MT/ha (Omar et al., 2019).

DATA COLLECTION

Sentinel-2 Temporal Imagery Data

The Sentinel-2 (S2) satellite constellation consists of two satellites, namely Sentinel-2A and Sentinel-2B. These satellites were launched by the European Space Agency (ESA) on 23 June 2015 (S2A) and 7 March 2017 (S2B), respectively. S2 satellites are equipped with a multispectral instrument (MSI) that acquires images with a swath width of 290 km and a spatial resolution ranging from 10-60 m (depending on the selected band). The S2 mission has a ten-day revisit time at the equator when utilising a single satellite and five days when the entire constellation is operational. (Xiao et al., 2021).

The Sentinel-2 Level-2A (Surface Reflectance, SR/ Bottom of Atmosphere (BOA)) images were not utilised in this study due to the presence of numerous artefacts and often being overcorrected, as noted by Brinkhoff et al. (2022) and Fatchurrachman et al. (2022). A recent study by Pascual-venter et al. (2024) suggests that TOA radiance has slightly better accuracy than BOA (SR) radiance. Pascual-venteo et al. (2024) also indicate that utilising TOA radiance can eliminate the need for complex atmospheric correction when retrieving vegetation traits, streamlining the process and potentially improving accuracy. Therefore, Sentinel-2 Level-1C (Top-of-Atmosphere Reflectance, TOA) images were chosen for this study.

Prior research has also documented the successful utilisation of Sentinel-2 Level-1C data for mapping paddy extent, such as in China (Ni et al., 2021; Shen et al., 2023) and Malaysia (Fatchurrachman et al., 2022). S2 L1C refers to Top-of-Atmosphere (TOA) reflectance image data that have been subject to radiometric and geometric corrections. These corrections encompass ortho-rectification and spatial registration on a global reference system, ensuring sub-pixel accuracy (European Space Agency, 2015; Google Developers, 2022).

Four bands from the S2 L1C TOA dataset were employed for computing the Normalised Difference Vegetation Index (NDVI) and Modified Normalised Difference Water Index (MNDWI). Band 4 (red) and 8 (near-infrared, NIR) were employed for computing NDVI, while band 3 (green) and band 11 (short-wave infrared 1 or SWIR1) were used to calculate MNDWI. The S2 TOA images possess a spatial resolution of 10 meters. S2 TOA temporal data were collected from January 2022 to October 2023, covering the study area's main and off seasons. A total of 3,900 scenes of S2-TOA temporal data were obtained from the Google Earth Engine (GEE) catalogue. GEE, a cloud-based platform for geospatial analysis (Gorelick et al., 2017), facilitated tasks such as data access, image pre-processing, vegetation index computation, area mapping, and calculations.

ESA WorldCover 10 m v100 2020

The ESA WorldCover 10m v100 was used to exclude non-cropland areas by masking out the cropland area (class value 40). Spurious data from other land cover types that could impact classification results were reduced, focusing on the cropland areas. The ESA WorldCover 10 m v 100 2020 dataset was generated based on the combination of Sentinel-1 and 2 temporal data as part of the ESA WorldCover project, which is a component of the 5th Earth Observation Envelope Programme (EOEP-5) by the European Space Agency. The product is a global land cover map for the year 2020 with a resolution of 10 meters, based on data from Sentinel-1 and Sentinel-2 satellites. The product contains 11 classes of land cover that include tree cover, shrubland, grassland, cropland, built-up, bare or sparse vegetation, snow and ice, permanent water bodies, herbaceous wetland, mangroves, moss and lichen (Google Developers, 2021; Zanaga et al., 2021).

Google Street View Images

Google Street View images accessed from Google Maps were utilised to verify the presence of rice fields in the classified area. Although the images were not acquired in 2022, they can still be used as indicators for the presence of rice fields in the classified area. Points of verification are accessible on the Google Earth Engine (GEE) platform (https://code.earthengine.google.com/7cb17f0460c4d9a00cc00787a28ec8a0).

Administrative Boundary

The administrative boundaries at both the State and District levels were acquired from the Global Administrative Unit Layers (GAUL) dataset provided by the Food and Agriculture Organization of the United Nations (FAO UN). The boundary data were accessed through the GEE catalogue using the command ee.FeatureCollection("FAO/GAUL/2015/level2").

Agricultural Statistics and Existing Rice Map

This study compared results using the Malaysia Paddy Production Survey (PPS) report published in 2021. The report collected estimates of yield, planted area and production for each season using probability sampling methods and objective measurements. These data were generated at the District, State and granary area levels (Department of Agriculture Peninsular Malaysia, 2021). The paddy parcel and harvested areas were compared with this study's estimates and presented in hectares (ha).

An existing rice map, NESEA-Rice10, was also compared with the results of this study (Table 1). NESEA-Rice 10 is a project that provides paddy rice maps for Northeast and Southeast Asia. It utilises a rule-based method combining temporal data of Sentinel-1 and MODIS satellite data to overcome the mixed-pixel challenge arising from coarse spatial

Table 1
Rice parcel area comparison between this study data, NESEA-Rice10 and statistic and its relative discrepancy

No	Districts	Rice parcel area by			Relative discrepancy	Relative discrepancy
		This study (ha)	NESEA-Rice10 (ha)	Statistic (ha)	(a) and (b)	(a) and (c)
		(a)	(b)	(c)	(%)	(%)
1	Besut	6,148	6,145	7,370	0.05	-16.58
2	Dungun	33	721	44	-95.42	-25.00
3	Hulu Terengganu	164	348	300	-52.87	-45.33
4	Kemaman	49	737	93	-93.35	-47.31
5	Kuala Terengganu	683	577	1,387	18.37	-50.76
6	Marang	208	455	792	-54.29	-73.74
7	Setiu	899	2,287	1,565	-60.69	-42.56
	Total	8,184	11,270	11,551	-27.38	-29.15

resolution. The dataset is publicly available at https://doi.org/10.5281/zenodo.5645344 (Han et al., 2021) and can be accessed for further analysis and decision-making.

METHODOLOGY

Figure 2 illustrates the workflow of the methodology employed in this study. The methodology framework employed in this study is referred to as the framework of phenology-expert-based unsupervised classification method (PEB-UC), which involves combining the k-means unsupervised method with expertise in rice phenology curves from Sentinel-2 data.

Data Pre-processing

Sentinel-2 TOA temporal data spanning from January 2022 to October 2023 were employed; These data were compiled and processed into the Monthly Maximum Value Composite (MaxVC) of NDVI and MNDWI. NDVI spectral was used to differentiate rice from other land covers and identify growth stages (Fatchurrachman et al., 2022; Ni et al., 2021). Meanwhile, MNDWI was used to detect the presence of standing water during the tillage and planting stage. In addition, although wet surfaces and built-ups have similar reflectance, MNDWI is capable of improving the differentiation between those two objects (Mansaray et al., 2019; Talema & Hailu, 2020). NDVI was calculated using Equation 1, employing band 4 (red) and band 8 (near-infrared). Meanwhile, MNDWI was calculated using Equation 2, employing band 3 (green) and band 11 (short-wave infrared 1 or SWIR1):

$$NDVI = \frac{band\ 8\ (NIR) - band\ 4\ (Red)}{band\ 8\ (NIR) + band\ 4\ (Red)} \quad [1]$$

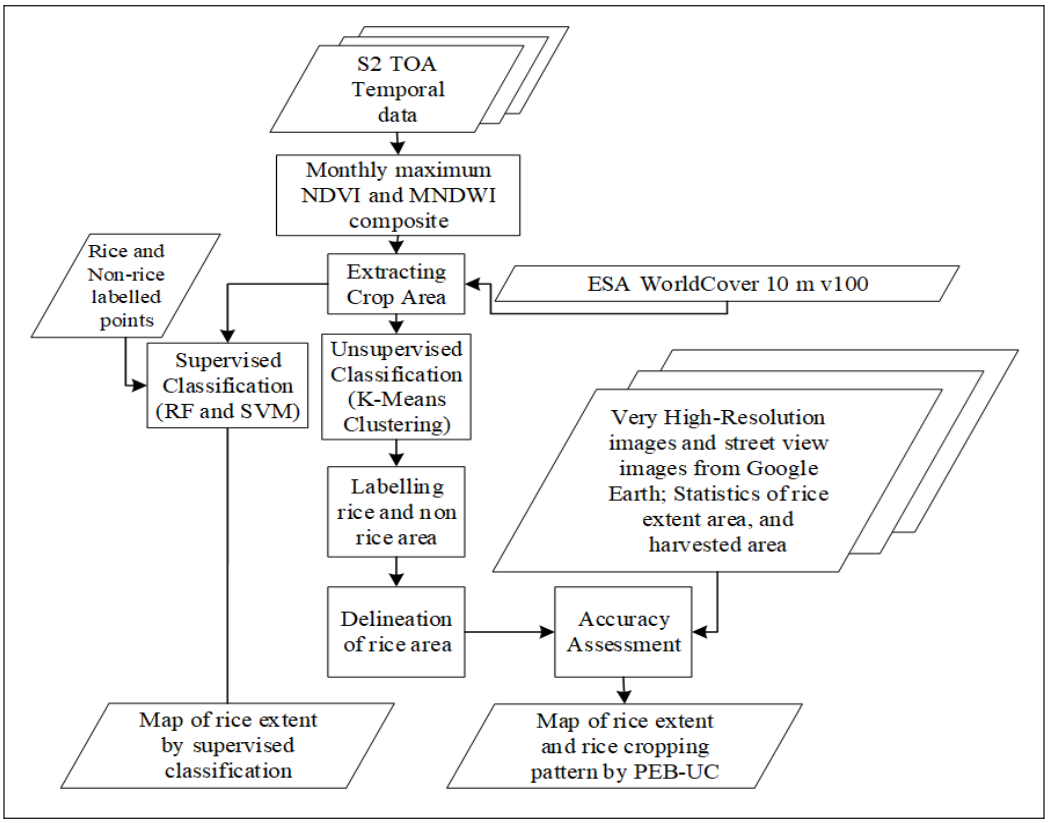

Figure 2. Workflow of the methodology in this study

$$MNDWI = \frac{band\ 3\ (Green) - band\ 11\ (SWIR1)}{band\ 3\ (Green) + band\ 11\ (SWIR1)} \quad [2]$$

Phenological studies using Sentinel-2 are limited by data gaps arising due to cloud cover, a prevalent issue with optical sensors (Misra et al., 2020). Additionally, optical Sentinel-2 data can be influenced by various factors, including changes in illumination and viewing conditions within and across images, fluctuations in atmospheric constituents such as water vapour and aerosol concentrations, as well as the presence of cloud cover (Holben, 1986). This study minimises these effects using maximum value composites (MaxVC) of the NDVI calculated from Sentinel-2 TOA temporal data from January 2022 to October 2023. MaxVC of the NDVI has proven effective in prior studies utilising MODIS, SPOT, and Sentinel-2 data (de Bie et al., 2012; Fatchurrachman et al., 2022; Gumma et al., 2014).

A compilation of 22 months of MaxVC NDVI and MNDWI datasets from January 2022 to October 2023 was stacked into a single image. First, we excluded non-cropland areas using the ESA WorldCover 10m v100 cropland band to reduce computational time, This procedure extracted rice fields from the classified cropland area and herbaceous area.

Concentrating on the cropland and herbaceous areas eliminated spurious data from other land cover area types that could impact classification results; it also significantly reduced computational cost and time.

Phenology-expert Based Unsupervised Classification Method (PEB-UC)

The pre-processed images served as inputs for the K-Means clustering model, implemented using the ee.Clusterer.wekaKMeans function within the GEE. This model employed a random-point sampling technique to establish centroids and produce clusters. Subsequently, these clusters were used to visually distinguish rice field and non-rice field areas based on characteristic spectral profiles derived from a monthly composite of NDVI and MNDWI temporal data.

Figure 3 illustrates the temporal evolution of the NDVI and MNDWI cluster profiles for four land covers: water bodies, built-up areas, trees and rice fields. Rice fields demonstrate a distinct temporal cluster profile characterised by seasonal fluctuations in NDVI values, while signals for other land covers remain relatively stable.

In detail, rice fields are flooded with water during the tillage and planting stage (T). Figure 3 depicts rice fields exhibiting a local minimum NDVI value during this period, while the MNDWI value reaches a maximum peak (F) (similar spectral of a water body or wet surface). Subsequently, as rice grows and canopy closure occurs in the vegetative (V) and reproductive (R) stages, increasing chlorophyll signals coincide with a significant decrease in soil signals (Ni et al., 2021). Consequently, NDVI value rapidly increased during this period, peaking at the end of the reproductive period. In contrast, the MNDWI value decreased until the maturity period (M) as the water content decreased.

A rapid decrease in chlorophyll content marks the maturity (M) period as the carotenoid content increases (Ni et al., 2021). This distinctive drop in NDVI values indicates the maturity of the rice plant, typically occurring in the last month of the rice growth cycle. Finally, NDVI values decreased due to biomass loss, signalling the harvest and fallow stages.

The representative cluster profiles of NDVI and MNDWI were visually identified, separating rice and non-rice field areas. We employed this method in our previous studies (Fatchurrachman et al., 2022; Rudiyanto et al., 2019) and successfully generated highly accurate maps of rice field extent.

Supervised Classification Model

In addition, we also performed supervised classification methods using random forest (RF) and support vector machine (SVM) to map rice parcel extent (growing area) in GEE. RF is an ensemble learning method that addresses the limitations of single decision trees by integrating many trees through a process called bootstrap aggregating (bagging) (Breiman, 2001). Meanwhile, SVM utilises a hyperplane to divide the support vectors and distinctly

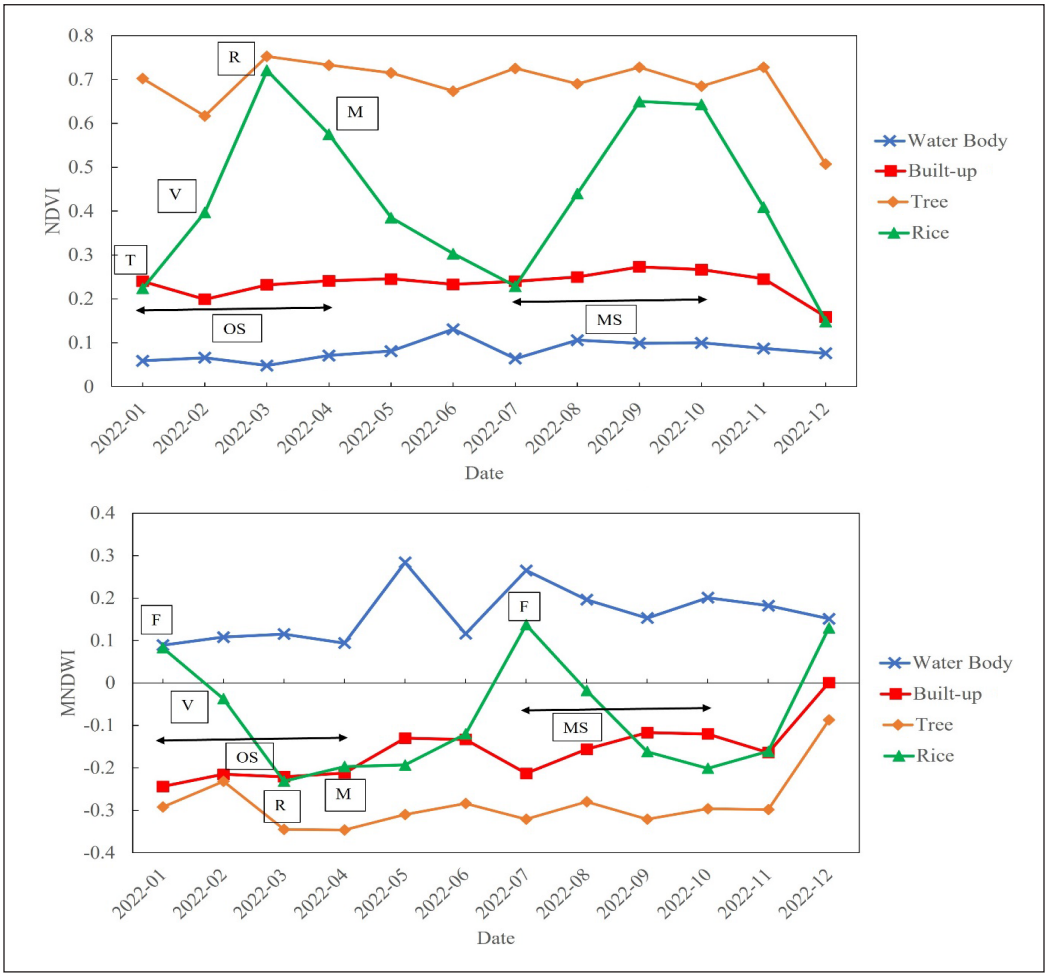

Figure 3. Temporal evolution of monthly composite NDVI and MNDWI cluster profile for four land-cover classes: water body, built-up, tree and rice field; T = tillage and planting, V = vegetative, R = reproductive, M = maturity, F = Flooding, OS = off-season, MS = main season

classify the data points (Maxwell et al., 2018). RF and SVM have built-in parameters that can be tuned to enhance their prediction performance. Based on trial and error, the number of tree parameters in the RF model was set to 30, while the SVM model used a radial basis function (RBF) kernel type with a gamma parameter of 0.5 and a cost of 10.

For training and validation of the models, 247 points (126 rice and 121 non-rice class) were visually labelled based on the very high-resolution image (VHRI) base map (i.e., satellite layer) in GEE and the Street View images in Google Maps. The observed data were randomly split into training and validation groups with a ratio of 8:2. For comparison, the same validation sample data were also used to check the validation accuracy of the PEB-UC classification results.

Accuracy Assessment

The agreement between the statistics of rice extent areas and the results obtained in this study was assessed using the coefficient of determination (R^2), as shown in Equation 3; the root mean square error (RMSE), as shown in Equation 4; and the percentage of relative discrepancy (%RD), as shown in Equation 5.

$$R^2 = 1 - \frac{\sum_{i=1}^{n}(y_{e-i} - y_{s-i})^2}{\sum_{i=1}^{n}(y_{s-i} - \mu)^2} \quad [3]$$

$$\text{RMSE} = \sqrt{\frac{\sum_{i=1}^{n}(y_{e-i} - y_{s-i})^2}{n}} \quad [4]$$

$$\%\ \text{RD} = \frac{(y_{e-i} - y_{s-i})}{y_{s-i}} \times 100 \quad [5]$$

Where y_e is the estimated rice extent from this study, and y_s is the rice extent from either statistical data or existing rice map of NESEA-Rice 10, subscript-$_i$ represents District, and n is the total Districts in Terengganu. Furthermore, the accuracy of the produced rice parcel extent maps from PEB-UC, RF and SVM models was also evaluated using overall accuracy and kappa coefficient through a contingency matrix for both the training and validation datasets.

RESULTS AND DISCUSSION

The PEB-UC proposed in this study is straightforward and resulted in rice parcel extent and rice cropping intensity through visual observation of the phenology of the spectral profile of Sentinel-2 time series data. Thus, we discussed the PEB-UC extensively in this study. Subsequently, we evaluated the comparison results between the PEB-UC and the two supervised methods (RF and SVM).

Distribution of Rice Extent and Cropping Schedule

Based on the labelled rice clusters extracted from the PEB-UC, rice extent or growing area across Terengganu was identified as shown in Figure 1 (https://rudiyanto.users.earthengine.app/view/riceterengganu). These rice extent areas were then calculated and presented at the district level. According to our findings, rice fields in Terengganu are dispersed across all districts. The total area of rice fields in Terengganu amounts to 8,184 hectares, with 53% (4,377 ha) situated within the IADA KETARA granary area exclusively in Besut District and the remaining 47% (3,807 ha) in non-granary areas distributed throughout the entire region. Figure 4 illustrates the distribution of the total rice fields (8,184 ha), where a significant portion of 75.12% (6,148 ha) of Terengganu's rice area is concentrated in Besut District, followed by Setiu 10.98% (899 ha), Kuala Terengganu (including Kuala Nerus)

8.35% (683 ha), Marang 2.54% (208 ha), Hulu Terengganu 2% (164 ha), and Kemaman 0.60% (49 ha), with Dungun having the smallest area at 0.40%, equivalent to 33 hectares.

Figure 5 showcases rice fields in Besut District, primarily situated along the northern Terengganu border with Kelantan State. The NDVI spectral profile indicates double cropping seasons, with rice planted in January and July. Most rice fields, constituting 71% of Besut's parcels, are within the IADA KETARA granary area, while 29% are in non-granary regions.

Only 24.9% of rice fields are situated beyond Besut District, with Dungun District featuring a singular planting area in Sungai Melung Sub-district (Supplementary Figure 1). Notably, based on the NDVI spectral profile, rice cultivation in this region occurs once

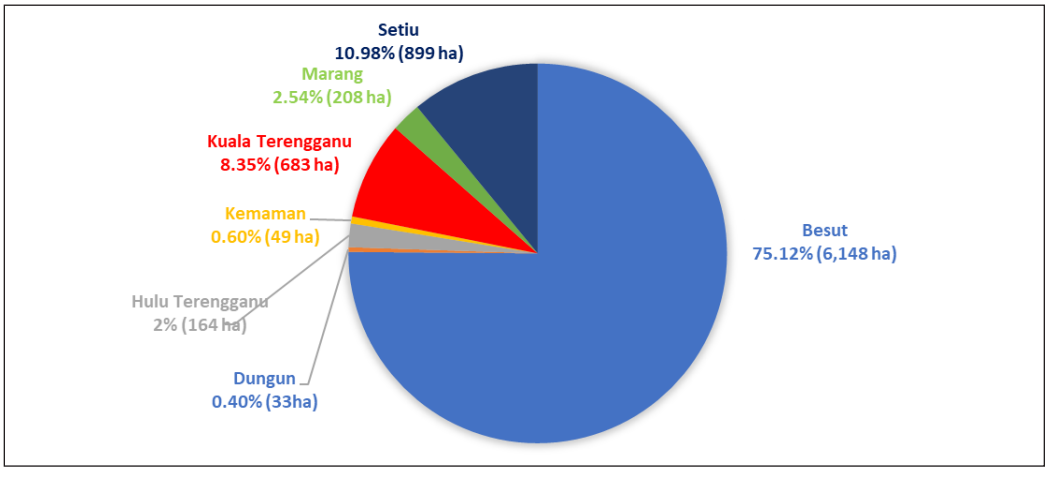

Figure 4. Percentage of Rice Field Extent at District level of Terengganu State, Malaysia

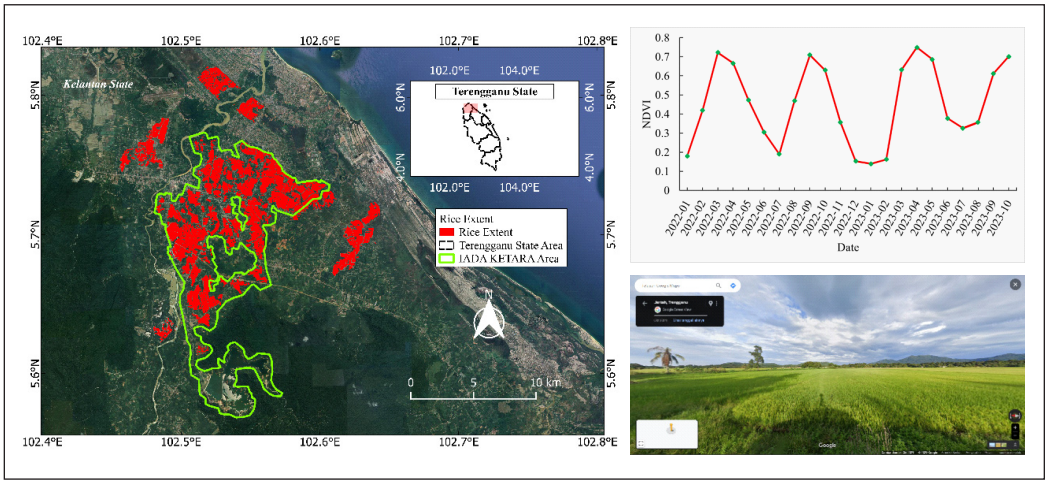

Figure 5. Rice extent at Besut District (red colour). The green colour line is the boundary area of IADA KETARA. © Google Street View image coordinate 102.50696604601183, 5.670731115164914

a year, specifically in April (2021) and February (2022). Moving on to Hulu Terengganu, rice cultivation spans across four sub-districts: Tok Lawit, Matang (Supplementary Figure 2a), Gaung, and Kemat (Supplementary Figure 2b), with planting occurring twice annually, in February and July. Similarly, Kemaman's rice cultivation is distributed across two sub-districts, Pasir Semut (Supplementary Figure 3a) and Dadong (Supplementary Figure 3b), both following a double cropping season with plantings in February and June, as depicted in the NDVI spectral profile, while fluctuations or sudden drops suggest the presence of clouds.

In Kuala Terengganu, encompassing Kuala Nerus, rice fields are dispersed across eleven sub-districts: Darat Batu Rakit, Tok Kulit, Padang Maras, Maras, Medan Cengal, Bukit Cempaka, Teluk Merbau, Bukit Wan (Supplementary Figure 4a), Tualang, Wakaf Mempelam, Gong Kemunting, and Alur Parit (Supplementary Figure 4b). Kuala Terengganu adopts a double cropping schedule, with rice planted in March and October. In Marang, rice cultivation is segmented across four sub-districts: Lubuk Pandan, Jerong Tuan, Bukit Kulim, and Bukit Jelulong (Supplementary Figure 5), adhering to a single cropping system with rice planted either in November or December. Lastly, in Setiu District, rice cultivation predominantly concentrates in the Permaisuri area, notably across four sub-districts: Gong Kubu, Kederang, Bukit Kemudu, and Buruk (Supplementary Figure 6a), alongside Alur Serdang Sub-district (Supplementary Figure 6b). Setiu operates on a double cropping system, with rice planted in January and September.

In summary, five districts—Besut, Hulu Terengganu, Kemaman, Kuala Terengganu, and Setiu—feature double cropping seasons in one year. Meanwhile, Dungun and Marang Districts adhere to a single cropping season within the same timeframe.

Comparison of Classification Results with Statistical Data and Existing Map Product

Table 1 compares the extent of rice parcel area in seven districts of Terengganu as determined by this study (2022), NESEA-Rice10 (2019), and agricultural statistics from 2021. The total area estimated for rice fields in this study is 8,184 hectares, compared to 11,270 hectares reported by NESEA-Rice10 and 11,551 hectares according to agricultural statistics in 2021. The map generated in this study shows a relative discrepancy of -29.15% from the agricultural statistics, whereas the discrepancy from NESEA-Rice10 is -27.38%. This discrepancy, particularly evident in the NESEA-Rice10 dataset, is attributed to the inclusion of non-rice areas being misclassified as rice fields, a phenomenon often referred to as the "salt and pepper effect." Due to the lack of spatial data, further investigation into this statistical disparity was not feasible.

Figures 6a and 6b show scatter plots of the agreement between the rice extent calculated from this study, agricultural statistics data, and the agreement between the NESEA-Rice10 estimates for 2019 (Han et al., 2021) and agricultural statistics data, respectively. This

study's estimated rice field extent had a higher correlation with agricultural statistics with a coefficient of determination $R^2 = 0.99$ and an RMSE of 632 ha (Figure 6). Meanwhile, the correlation of the NESEA-Rice10 map with agricultural statistic data was $R^2 = 0.93$ and RMSE of 732 ha (Figure 6b). By comparison, this study has a better agreement than the NESEA-Rice10 map product to the statistical data.

Table 2 lists the rice harvested area across seven districts of Terengganu generated from this study compared with agricultural statistics from 2021. Based on the results, the study data and the statistics indicate that the harvested area during the main seasons is larger than during the off-season. The number of seasons identified in this study data aligns well

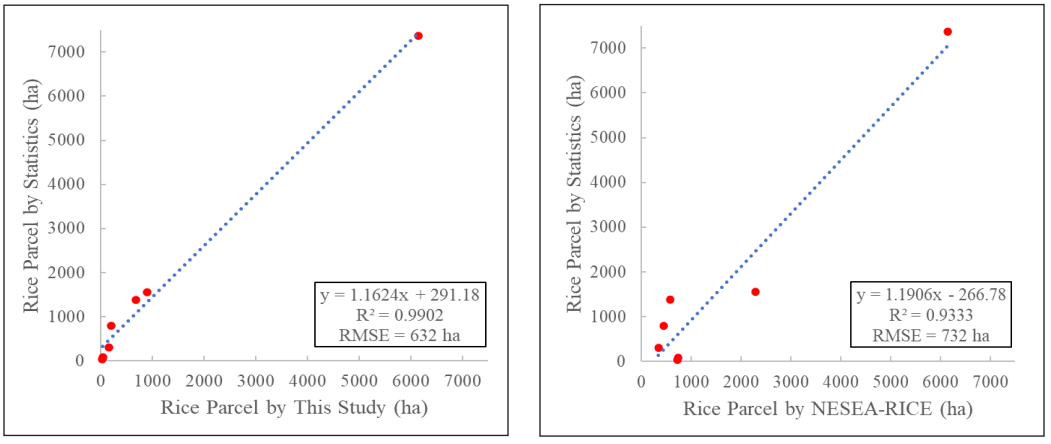

(a) (b)

Figure 6. Comparison between rice area estimates derived from (a) this study and statistical data (District level) and (b) NESEA-Rice10 data and statistical data (District level)

Table 2
The harvested rice area and number of seasons are compared using this study's data and statistics

No	Districts	This Study			Statistic		
		Harvested Area (ha)		Number of Season per year	Harvested Area (ha)		Number of Season per year
		Off Season	Main Season		Off Season	Main Season	
1	Besut	6,148	6,148	2	7,095	7,095	2
2	Dungun	0	33	1	0	33	1
3	Hulu Terengganu	164	164	2	120	193	2
4	Kemaman	49	49	2	58	58	2
5	Kuala Terengganu	683	683	2	377	1,167	2
6	Marang	0	208	1	0	509	1
7	Setiu	899	899	2	1,448	1,448	2
	Total	7,943	8,184		9,098	10,503	

with the 2021 statistics. Overall, the study data underestimate the harvested areas during both off-season and main seasons compared to the statistical data from 2021.

Comparison between PEB-UC and Supervised Classification

Accuracy of Classification Models

The accuracy assessment between the PEB-UC, RF, and SVM classification models is listed in Supplementary Table 1. The PEB-UC classification result was validated using the same validation sample points as the supervised models. The overall accuracy for the validation of PEB-UC was 0.979, with a kappa coefficient of 0.957, which is higher compared to both RF (overall accuracy = 0.875 and kappa = 0.743) and SVM (overall accuracy = 0.937 and kappa = 0.870). PEB-UC outperformed both supervised methods because the two supervised methods showed relatively high overfitting, as indicated by a training overall accuracy of 1 and a kappa coefficient of 1 (Supplementary Table 1).

Comparison of Rice Parcel Area and Quality of Rice Map

Comparison of rice parcel areas between PEB-UC, RF, SVM, and statistics, along with their relative discrepancies, are presented in Supplementary Table 2. PEB-UC estimated 8,184 ha, RF 8,428 ha, and SVM 7,966 ha. Compared to 2021 agricultural statistics (11,551 hectares), the relative discrepancies were -29.15% for PEB-UC, -27.04% for RF, and -31.04% for SVM. The PEB-UC rice map also shows more dense and clear separability between rice and non-rice (roads, irrigation channels, built-up areas, and other vegetation covers) compared to both supervised models, as shown in the comparison map available at https://rudiyanto.users.earthengine.app/view/riceterengganu.

Figure 7. Example of error in rice field classification: The red colour shows an area classified as a rice field, while the RGB colour is the non-rice areas in Besut District (102.45713 E, 5.74593 N)

Uncertainty Source

The current study has successfully produced a highly accurate map of rice extent. Nonetheless, it is essential to acknowledge certain potential limitations. Common errors occur at the boundary zones between rice and non-rice fields. The mixed pixel effect at these boundary zones contributed to this discrepancy, as illustrated in Figure 7. This effect, documented in previous rice mapping studies, remains a

significant source of spatial uncertainty (Clauss et al., 2016; M Wang et al., 2022; Mo Wang et al., 2022). Commission errors, where non-rice areas are misclassified as rice fields, were primarily attributed to unwell-managed rice blocks being detected as rice.

CONCLUSION

The Phenology-Expert Based Unsupervised Classification Method (PEB-UC), using Sentinel-2 time series imagery data on the Google Earth Engine platform, has successfully generated a high-resolution (10 m) map of rice extent across Terengganu, Malaysia. This approach also offers cropping calendars based on monthly NDVI spectral profiles. The study reveals that the total rice extent in Terengganu is 8,184 hectares, with 53% situated in the IADA KETARA granary area and the remaining portion spread across non-granary areas. At the district level, the estimated rice field extent correlates strongly with agricultural statistics ($R^2 = 0.99$, RMSE = 632 ha), and the number of cropping seasons per year in this study aligns well with the statistics. The overall accuracy for the validation of PEB-UC was 0.979, with a kappa coefficient of 0.957, which outperformed both RF and SVM models. The PEB-UC rice map also shows more dense and clear separability between rice and non-rice compared to both supervised models. These insights into the spatial and temporal patterns of rice cultivation in Terengganu are valuable for policy formulation by the Department of Agriculture (DOA) Malaysia. Additionally, these spatial data complement agricultural statistical data, frequently presented as tabulated numerical data only.

ACKNOWLEDGEMENT

This study received support from the Talent & Publication Enhancement-Research Grant (TAPE-RG) Dana Penyelidikan Universiti Malaysia Terengganu (DP–UMT), under grant number UMT/TAPE-RG/2020/55246.

REFERENCES

Ali, A. M., Savin, I., Poddubskiy, A., Abouelghar, M., Saleh, N., Abutaleb, K., El-Shirbeny, M., & Dokukin, P. (2021). Integrated method for rice cultivation monitoring using sentinel-2 data and leaf area index. *Egyptian Journal of Remote Sensing and Space Science*, *24*(3), 431–441. https://doi.org/10.1016/j.ejrs.2020.06.007

Breiman, L. (2001). Random forest. *Machine Learning, 45*, 5–32. https://doi.org/10.1007/978-3-030-62008-0_35

Brinkhoff, J., Houborg, R., & Dunn, B. W. (2022). Rice ponding date detection in Australia using sentinel-2 and planet fusion imagery. *Agricultural Water Management*, *273*, Article 107907. https://doi.org/10.1016/j.agwat.2022.107907

Clauss, K., Yan, H., & Kuenzer, C. (2016). Mapping paddy rice in China in 2002, 2005, 2010 and 2014 with MODIS time series. *Remote Sensing*, *8*(5), Article 434. https://doi.org/10.3390/rs8050434

de Bie, C. A. J. M. D., Nguyen, T. T. H., Ali, A., Scarrott, R., & Skidmore, A. K. (2012). LaHMa: A landscape heterogeneity mapping method using hyper-temporal datasets. *International Journal of Geographical Information Science*, *26*(11), 2177–2192. https://doi.org/10.1080/13658816.2012.712126

Department of Agriculture Peninsular Malaysia. (2021). *Paddy production survey report Malaysia*. Department of Agriculture Peninsular Malaysia. https://www.doa.gov.my/doa/resources/aktiviti_sumber/sumber_awam/maklumat_pertanian/perangkaan_tanaman/laporan_penyiasatan_padi_musim_utama_2020_2021.pdf

European Space Agency. (2015). *Sentinel-2 user handbook*. European Space Agency (ESA). https://doi.org/10.1021/ie51400a018

Fatchurrachman, Rudiyanto, Soh, N. C., Shah, R. M., Giap, S. G. E., Setiawan, B. I., & Minasny, B. (2022). High-Resolution mapping of paddy rice extent and growth stages across peninsular malaysia using a fusion of sentinel-1 and 2 time series data in google earth engine. *Remote Sensing*, *14*(8), Article 1875. https://doi.org/10.3390/rs14081875

Feng, F., Gao, M., Liu, R., Yao, S., & Yang, G. (2023). A deep learning framework for crop mapping with reconstructed sentinel-2 time series images. *Computers and Electronics in Agriculture*, *213*, Article 108227. https://doi.org/10.1016/j.compag.2023.108227

Google Developers. (2021). *ESA worldcover 10m v100*. Google Developers. https://developers.google.com/earth-engine/datasets/catalog/ESA_WorldCover_v100

Google Developers. (2022). *Sentinel-2*. Google Developers.

Gorelick, N., Hancher, M., Dixon, M., Ilyushchenko, S., Thau, D., & Moore, R. (2017). Remote sensing of environment google earth engine : Planetary-scale geospatial analysis for everyone. *Remote Sensing of Environment*, *202*, 18–27. https://doi.org/10.1016/j.rse.2017.06.031

Griffiths, P., Nendel, C., & Hostert, P. (2019). Intra-annual reflectance composites from sentinel-2 and landsat for national-scale crop and land cover mapping. *Remote Sensing of Environment*, *220*, 135–151. https://doi.org/10.1016/j.rse.2018.10.031

Gumma, M. K., Thenkabail, P. S., Maunahan, A., Islam, S., & Nelson, A. (2014). Mapping seasonal rice cropland extent and area in the high cropping intensity environment of Bangladesh using MODIS 500m data for the year 2010. *ISPRS Journal of Photogrammetry and Remote Sensing*, *91*, 98–113. https://doi.org/10.1016/j.isprsjprs.2014.02.007

Han, J., Zhang, Z., Luo, Y., Cao, J., Zhang, L., Cheng, F., Zhuang, H., Zhang, J., & Tao, F. (2021). NESEA-Rice10: High-resolution annual paddy rice maps for Northeast and Southeast Asia from 2017 to 2019. *Earth System Science Data*, *13*(12), 5969–5986. https://doi.org/10.5194/essd-13-5969-2021

Han, J., Zhang, Z., Luo, Y., Cao, J., Zhang, L., & Zhuang, H. (2022). Annual paddy rice planting area and cropping intensity datasets and their dynamics in the Asian monsoon region from 2000 to 2020. *Agricultural Systems*, *200*, Article 103437. https://doi.org/10.1016/j.agsy.2022.103437

Hashim, M. F. C., Nurulhuda, K., Haidar, A. N., Muharam, F. M., Nurulhuda, K., Berahim, Z., Ismail, M. R., Zad, S. N. M., & Zulkafli, Z. (2022). Physiological and yield responses of five rice varieties to nitrogen fertilizer under farmer's field in IADA Ketara, Terengganu, Malaysia. *Sains Malaysiana*, *51*(2), 359–368. https://doi.org/10.17576/jsm-2022-5102-03

Holben, B. N. (1986). Characteristics of maximum-value composite images from temporal AVHRR data. *International Journal of Remote Sensing*, *7*(11), 1417–1434. https://doi.org/10.1080/01431168608948945

Jiang, Q., Tang, Z., Zhou, L., Hu, G., Deng, G., Xu, M., & Sang, G. (2023). Mapping paddy rice planting area in dongting lake area combining time series sentinel-1 and sentinel-2 images. *Remote Sensing*, *15*(11), Article 2794. https://doi.org/10.3390/rs15112794

Liu, Y., Xiao, D., & Yang, W. (2022). An algorithm for early rice area mapping from satellite remote sensing data in southwestern Guangdong in China based on feature optimization and random Forest. *Ecological Informatics*, *72*, Article 101853. https://doi.org/10.1016/j.ecoinf.2022.101853

Mansaray, L. R., Yang, L., Kabba, V. T. S., Kanu, A. S., Huang, J., & Wang, F. (2019). Optimising rice mapping in cloud-prone environments by combining quad-source optical with sentinel-1A microwave satellite imagery. *GIScience and Remote Sensing*, *56*(8), 1333–1354. https://doi.org/10.1080/15481603.2019.1646978

Maxwell, A. E., Warner, T. A., & Fang, F. (2018). Implementation of machine-learning classification in remote sensing: An applied review. *International Journal of Remote Sensing*, *39*(9), 2784–2817. https://doi.org/10.1080/01431161.2018.1433343

Ministry of Economy Malaysia. (2023). *Mid Term Review Twelve Malaysia Plan 2021-2025 Malaysia Madani: Sustainable, Prosperous, High Incom*e. Ministry of Economy.

Misra, G., Cawkwell, F., & Wingler, A. (2020). Status of phenological research using sentinel-2 data: A review. *Remote Sensing*, *12*(17), 10–14. https://doi.org/10.3390/RS12172760

Ni, R., Tian, J., Li, X., Yin, D., Li, J., Gong, H., Zhang, J., Zhu, L., & Wu, D. (2021). An enhanced pixel-based phenological feature for accurate paddy rice mapping with Sentinel-2 imagery in Google Earth Engine. *ISPRS Journal of Photogrammetry and Remote Sensing*, *178*, 282–296. https://doi.org/10.1016/j.isprsjprs.2021.06.018

Omar, S. C., Shaharudin, A., & Siti, A. T. (2019). *The status of the paddy and rice industry in Malaysia.* Khazanah Research Institute.

Omia, E., Bae, H., Park, E., Kim, M. S., Baek, I., Kabenge, I., & Cho, B. K. (2023). Remote sensing in field crop monitoring: A comprehensive review of sensor systems, data analyses and recent advances. *Remote Sensing*, *15*(2), Article 354. https://doi.org/10.3390/rs15020354

Padarian, J., Minasny, B., & McBratney, A. B. (2020). Machine learning and soil sciences: A review aided by machine learning tools. *Soil*, *6*(1), 35–52. https://doi.org/10.5194/soil-6-35-2020

Pascual-venteo, A. B., Garcia, J. L., Berger, K., Estévez, J., Vicent, J., Pérez-suay, A., Wittenberghe, S. Van, & Verrelst, J. (2024). Gaussian process regression hybrid models for the top-of-atmosphere retrieval of vegetation traits applied to PRISMA and EnMAP imagery. *Remote Sensing*, *16*(7), Article 1211. https://doi.org/10.3390/rs16071211

Qiu, B., Yu, L., Yang, P., Wu, W., Chen, J., Zhu, X., & Duan, M. (2024). Mapping upland crop–rice cropping systems for targeted sustainable intensification in South China. *Crop Journal*, *12*(2), 614–629. https://doi.org/10.1016/j.cj.2023.12.010

Raju, C., Krishnapillai, A., Pillai, A. B., Sarala, A., & Divya, V. (2022). Rice area mapping in Palakkad district of Kerala using sentinel - 2 data and geographic information system technique. *Journal of Applied and Natural Science*, *14*(4), 1360–1366. https://doi.org/10.31018/jans.v14i4.3898

Ramadhani, F., Pullanagari, R., Kereszturi, G., & Procter, J. (2020). Automatic mapping of rice growth stages using the integration of sentinel-2, mod13q1, and sentinel-1. *Remote Sensing*, *12*(21), Article 3613. https://doi.org/10.3390/rs12213613

Rauf, U., Qureshi, W. S., Jabbar, H., Zeb, A., Mirza, A., Alanazi, E., Khan, U. S., & Rashid, N. (2022). A new method for pixel classification for rice variety identification using spectral and time series data from sentinel-2 satellite imagery. *Computers and Electronics in Agriculture*, *193*, Article 106731. https://doi.org/10.1016/j.compag.2022.106731

Rudiyanto, Minasny, B., Shah, R. M., Soh, N. C., Arif, C., & Setiawan, B. I. (2019). Automated near-real-time mapping and monitoring of rice extent, cropping patterns, and growth stages in Southeast Asia using sentinel-1 time series on a Google Earth Engine platform. *Remote Sensing*, *11*(14), Article 1666. https://doi.org/10.3390/rs11141666

Setiyono, T. D., Quicho, E. D., Holecz, F. H., Khan, N. I., Romuga, G., Maunahan, A., Garcia, C., Rala, A., Raviz, J., Collivignarelli, F., Gatti, L., Barbieri, M., Phuong, D. M., Minh, V. Q., Vo, Q. T., Intrman, A., Rakwatin, P., Sothy, M., Veasna, T., … & Mabalay, M. R. O. (2018). Rice yield estimation using synthetic aperture radar (SAR) and the ORYZA crop growth model: Development and application of the system in South and South-east Asian countries. *International Journal of Remote Sensing*, *40*(21), 8093–8124. https://doi.org/10.1080/01431161.2018.1547457

Shen, R., Pan, B., Peng, Q., Dong, J., Chen, X., Zhang, X., Ye, T., Huang, J., & Yuan, W. (2023). High-resolution distribution maps of single-season rice in China from 2017 to 2022. *Earth System Science Data*, *15*(7), 3203–3222. https://doi.org/10.5194/essd-15-3203-2023

Suratman, S., Sailan, M. I. M., Hee, Y. Y., Bedurus, E. A., & Latif, M. T. (2015). A preliminary study of water quality index in Terengganu River basin, Malaysia. *Sains Malaysiana*, *44*(1), 67–73. https://doi.org/10.17576/jsm-2015-4401-10

Talema, T., & Hailu, B. T. (2020). Mapping rice crop using sentinels (1 SAR and 2 MSI) images in tropical area: A case study in Fogera wereda, Ethiopia. *Remote Sensing Applications: Society and Environment*, *18*, Article 100290. https://doi.org/10.1016/j.rsase.2020.100290

Thorp, K. R., & Drajat, D. (2021). Deep machine learning with Sentinel satellite data to map paddy rice production stages across West Java, Indonesia. *Remote Sensing of Environment*, *265,* Article 112679. https://doi.org/10.1016/j.rse.2021.112679

Tiwari, V., Tulbure, M. G., Caineta, J., Gaines, M. D., Perin, V., Kamal, M., Krupnik, T. J., Aziz, M. A., & Islam, A. F. M. T. (2024). Automated in-season rice crop mapping using sentinel time-series data and Google Earth Engine : A case study in climate-risk prone Bangladesh. *Journal of Environmental Management*, *351*, Article 119615. https://doi.org/10.1016/j.jenvman.2023.119615

Wang, G., Meng, D., Chen, R., Yang, G., Wang, L., Jin, H., Ge, X., & Feng, H. (2024). Automatic rice early-season mapping based on simple sensing images. *Remote Sensing, 16*(2), Article 277. https://doi.org/10.3390/rs16020277

Wang, M., Wang, J., Chen, L., & Du, Z. (2022). Mapping paddy rice and rice phenology with sentinel-1 SAR time series using a unified dynamic programming framework. *Open Geosciences*, *14*(1), 414–428. https://doi.org/10.1515/geo-2022-0369

Wang, M., Wang, J., Cui, Y., Liu, J., & Chen, L. (2022). Agricultural field boundary delineation with satellite image segmentation for high-resolution crop mapping: A case study of rice paddy. *Agronomy*, *12*(10), Article 2342. https://doi.org/10.3390/agronomy12102342

Xiao, W., Xu, S., & He, T. (2021). Mapping paddy rice with sentinel-1/2 and phenology-, object-based algorithm - A implementation in Hangjiahu Plain in China using GEE platform. *Remote Sensing*, *13*(5), Article 990. https://doi.org/10.3390/rs13050990

Zanaga, D., Kerchove, R. V. D., Keersmaecker, W. D., Souverijns, N., Brockmann, C., Quast, R., Wevers, J., Grosu, A., Paccini, A., Vergnaud, S., Cartus, O., Santoro, M., Fritz, S., Georgieva, I., Lesiv, M., Carter, S., Herold, M., Li, L., Tsendbazar, N. E., … Arino, O. (2021). *ESA World Cover 10m 2020 v100*. European Space Agency (ESA). https://doi.org/10.5281/zenodo.5571936

Zhao, R., Li, Y., & Ma, M. (2021). Mapping paddy rice with satellite remote sensing: A review. *Sustainability*, *13*(2), Article 503. https://doi.org/10.3390/su13020503

APPENDIX

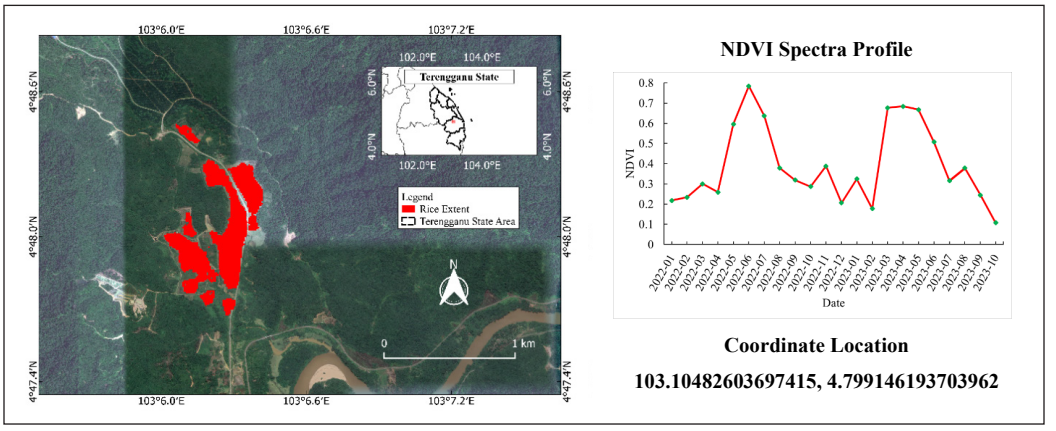

Supplementary Figure 1. Rice extent at Dungun District. Rice location coordinates 103.10482603697415, 4.799146193703962

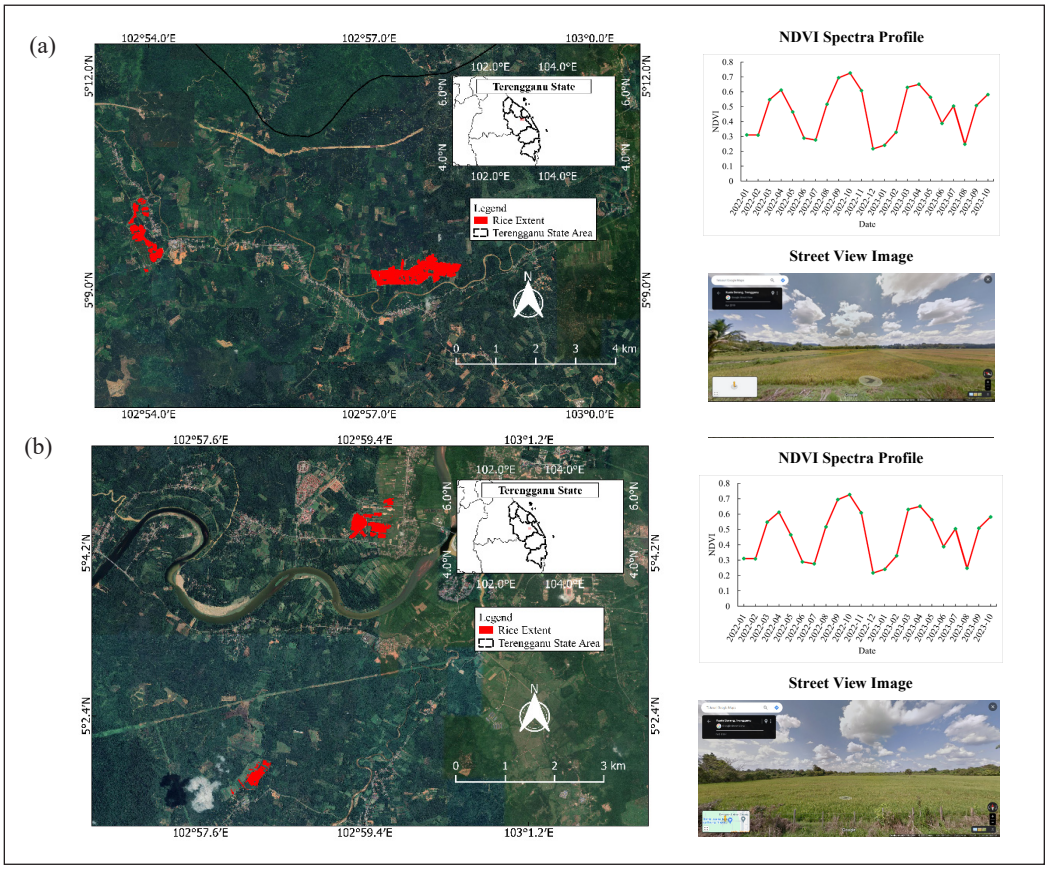

Supplementary Figure 2. Rice extent at Hulu Terengganu District: (a) Tok Lawit and Matang Sub-district, (b) Gaung and Kemat Sub-district. © Google Street View image coordinate: (a) 102.89854868916677, 5.15998499939375; (b) 102.98815719945003, 5.074533627188336

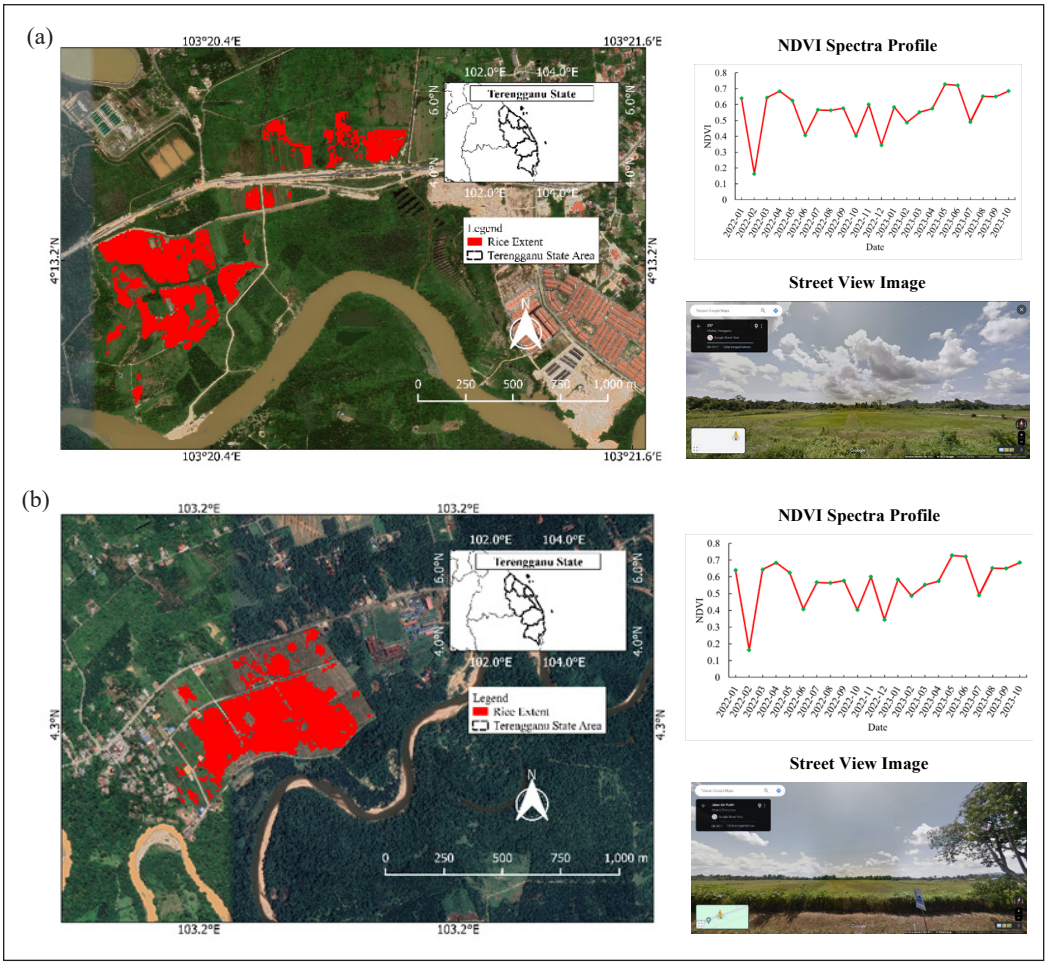

Supplementary Figure 3. Rice extent at Kemaman District: (a) Pasir Semut Sub-district; (b) Dadong Sub-district, © Google Street View image coordinate: (a) 103.34212221711789; 4.223077206270977 (b) 103.23149627791656, 4.282389429361505

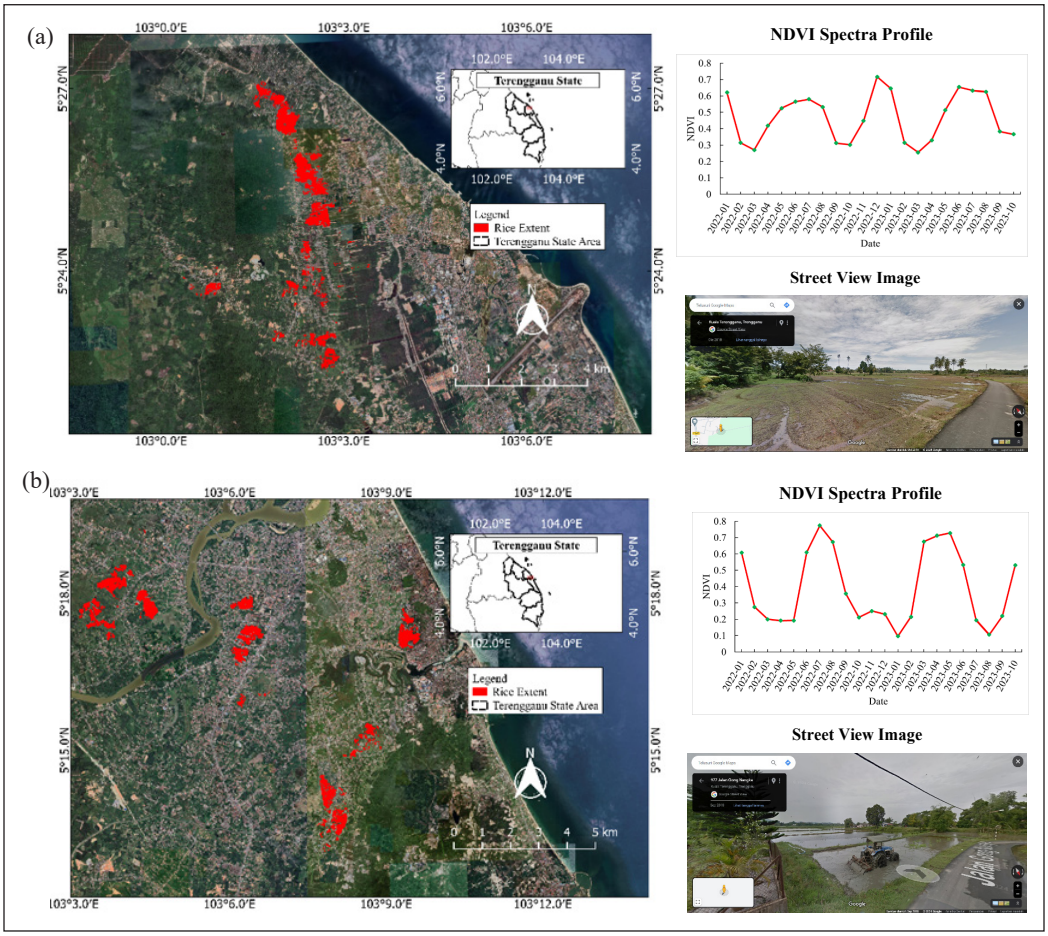

Supplementary Figure 4. Rice extent at Kuala Terengganu District: (a) Darat Batu Rakit, Tok Kulit, Padang Maras, Maras, Medan Cengal, Bukit Cempaka, Teluk Merbau, Bukit Wan Sub-districts; (b) Tualang, Wakaf Mempelam, Gong Kemunting, and Alur Parit Sub-districts, © Google Street View image coordinate (a) 103.04158359086921, 5.41650121980068 (b) 103.15765153308007, 5.289039091455927

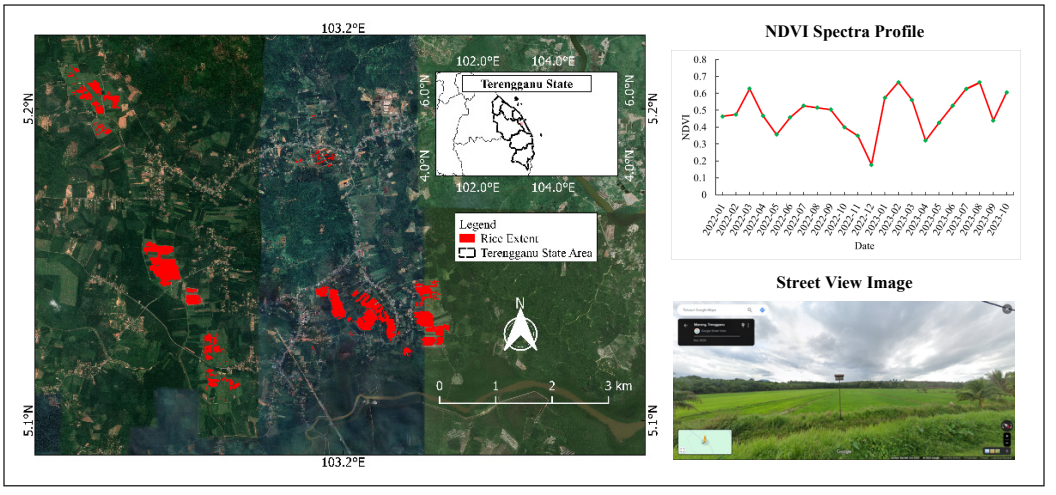

Supplementary Figure 5. Rice extent at Marang District. © Google Street View image coordinate 103.1121499235461, 5.146720931152082

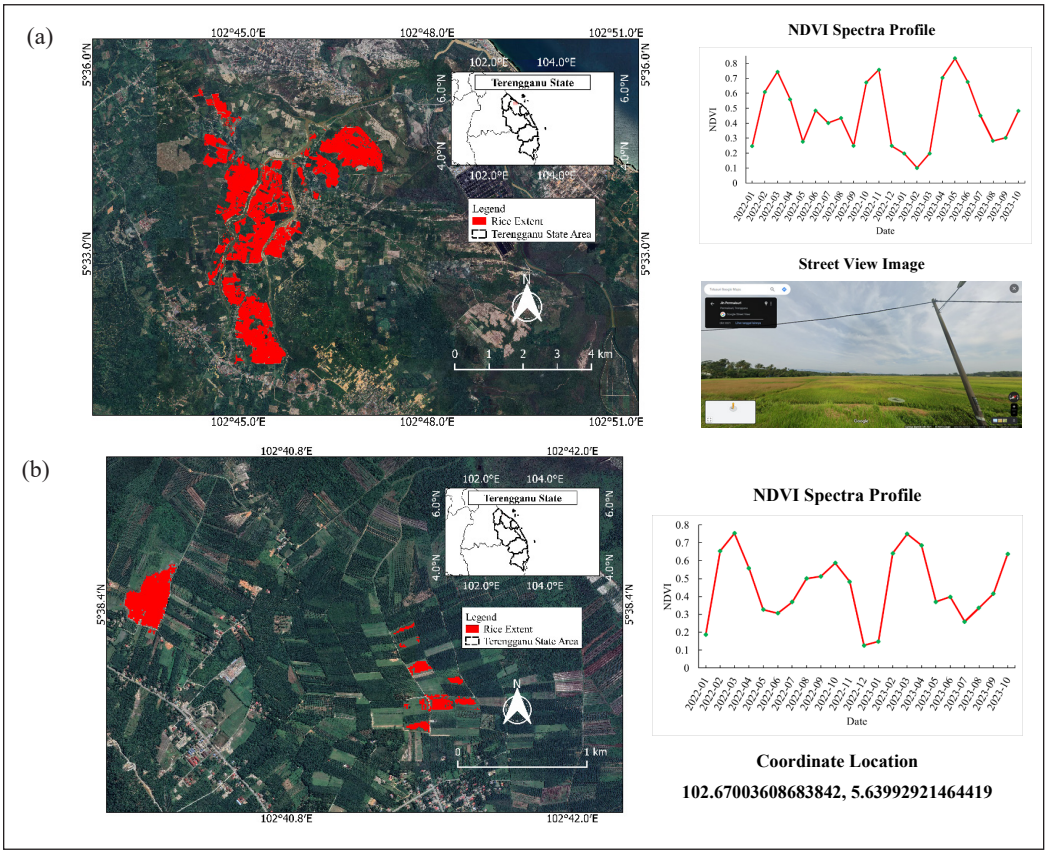

Supplementary Figure 6. Rice extent at Setiu District; (a) Gong Kubu, Kederang, Bukit Kemudu, and Buruk Sub-district, (b) Alur Serdang Sub-district, © Google Street View image coordinate (a) 102.75026252196312, 5.536907633129734 (b) 102.67003608683842, 5.63992921464419

Supplementary Table 1
Accuracy comparison of classification models: PEB-UC, RF and SVM

Method	Training		Validation	
	Overall Accuracy	**Kappa Coefficient**	**Overall Accuracy**	**Kappa Coefficient**
PEB-UC	-	-	0.979	0.957
RF	1.000	1.000	0.875	0.743
SVM	1.000	1.000	0.937	0.870

Supplementary Table 2
Rice parcel area comparison between this study data (PEB-UC), RF, SVM and statistics and its relative discrepancy

Rice Parcel Area by (ha)				Relative discrepancy		
PEB-UC (a)	**RF (b)**	**SVM (c)**	**Statistic (d)**	**(a) and (d) (%)**	**(b) and (d) (%)**	**(c) and (d) (%)**
8,184	8,428	7,966	11,551	-29.15	-27.04	-31.04